Vesicle Distribution in Glaciovolcanic Pillow Lava from Undirhlíðar, Southwest Iceland

Anna C. Thompson
Senior Integrative Exercise
March 10, 2017

Submitted in partial fulfillment of the requirements for a Bachelor of Arts degree from Carleton College, Northfield, Minnesota.

CONTENTS

Abstract

Introduction…….……....1
Geology of Iceland and Glaciovolcanology……...……1
Field Area….……..4
Pillow Lava Morphology…….…...5
Vesicle Distribution.……...7

Methods……...…….....8
Field Work……..8
Image Processing……..10
Hand Samples…...…….…...14
Vertical Distribution Model……..15

Results……..17
Pillow-Scale Observations……17
ImageJ Analysis……18
Geochemistry and Thin Sections……..23
Vertical Distribution Model……..23

Discussion……....28
Interpretation of Pillow Types……..28
Vesicle Rings……..…..30
Vertical Distribution Model……..32

Conclusion……...32

Acknowledgements…….33

References……33

Vesicle Distribution in Glaciovolcanic Pillow Lava from Undirhlíðar, Southwest Iceland

Anna C. Thompson
Carleton College
Senior Integrative Exercise
March 10, 2017

Carleton Advisor:
Cameron Davidson

Keck Advisors:
Meagen Pollock, College of Wooster
Ben Edwards, Dickinson College

ABSTRACT

Pillow lava is the most common lava morphology on Earth. It is found in high abundance in many environments, from the ocean floor to the surface of Mars. Because pillow lava forms during subaqueous eruptions, it is often inaccessible for study. Thus, being able to analyze pillow lava using visible physical characteristics without requiring samples could improve pillow lava research. This paper analyzes the distribution and emplacement mechanisms of vesicles in uniquely accessible pillow lavas found in Undirhlíðar Quarry. These pillows are the only lasting record of a preexisting englacial lake formed during a subglacial eruption, so understanding the details of their vesicles may provide new insights into the timing and nature of their emplacement. I propose that the type of vesicle distribution in a pillow cross section may be used to infer proximity to the source, the rate at which the pillow cooled, and eruption events during pillow emplacement. In this study, I define six types of vesicle distribution in pillow lava based on the presence of a vesiculated core, vesicles in the body, and a hollow pocket. Four pillow types were identified in the field. The observed pillow types all had vesiculated bodies but different cores. I propose that vesiculated cores are the result of rapid pressure changes, that non-vesiculated cores indicate slow cooling and proximity to the source, and that hollow pockets indicate that the source was cut off or diverted. Vesicle rings and cores may be indicative of different events, like magma pulses or sudden changes of pressure of the surrounding environment.

Keywords: pillow lava, vesicular texture, subglacial lake, volcanology, Iceland, Reykjanes Ridge

INTRODUCTION

Subglacial volcanism is common in Iceland, the Antarctic Peninsula, and parts of British Columbia. These eruptions melt englacial lakes that provide subaqueous environments for pillow lava emplacement (Pollock et al., 2014). Although pillow lava is one of the most abundant lava morphologies on Earth, it is relatively inaccessible because of its submarine or subglacial eruption environments and its presence on other planets, like Mars (Allen, 1979). Thus, being able to analyze pillow lava using visible physical characteristics without requiring samples would improve pillow lava research. Undirhlíðar Quarry, in southwest Iceland, provides unique access to thousands of pillows because it exposes a partly dissected volcano that formed under Pleistocene glaciers that have since receded. This paper analyzes the distribution and emplacement mechanisms of vesicles in pillow lavas found in the walls of Undirhlíðar Quarry. These pillow lavas are the only lasting record of a preexisting englacial lake, presumably formed during a subglacial eruption, so understanding the details of their vesicles may provide new insights into the timing and nature of their emplacement.

Geology of Iceland and Glaciovolcanology

Iceland lies over the Mid-Atlantic Ridge, where the North American and European Plates are spreading at a half rate of 0.9 cm per year N110E (Bourgeois, 1998). Iceland is further buoyed above sea level by the young basalt supplied by an underlying mantle plume (Guðmundsson, 2005). These principal sources of young basalt were initiated about 24 Ma and fuel Iceland's volcanism, which includes almost every known volcano type and eruption style on Earth (Thordarson and Larsen, 2007). The resulting Iceland basalt plateau rises over 3,000 m above the surrounding sea floor and covers

350,000 km^2. Only 30 % of this area is the island of Iceland itself, and the remaining area makes up the surrounding 50-200 km wide submarine shelf (Thordarson and Larsen, 2007).

Glaciations are thought to have covered Iceland completely and extended beyond the present coast several times at their maximum extent in the Pleistocene (Guðmundsson, 2005). Today, about 11 % of Iceland is covered by icecaps (Fig. 1) that existed through most of the Holocene (Guðmundsson, 2005). Subglacial eruptions are dominant in Iceland, even though glacial loading dampens magma production rates (Jull and McKenzie, 1996; Sigmarsson and Steinthórsson, 2007; Sigvaldason et al., 1992). Glaciovolcanic formations are created by a complicated series of eruptions in changing ice confined environments and are rarely exclusively subglacial (Guðmundsson, 2005). Most often, subglacial eruptions break through the ice and become emergent phreatomagmatic eruptions (Guðmundsson, 2005; Pollock et al., 2014).

Volcanic ridges and table mountains called tindars and tuyas are the subglacial equivalents of shield volcanoes and subaerial eruptive fissures (Bourgeois, 1998). They are composed of up to 50 km^3 of pillow lava, breccia, and hyaloclastite and are up to 35 km long (Guðmundsson, 2005). Tindars and tuyas are thought to form over a period of years or decades from an evolving source in a complicated series of eruptive episodes (Pollock et al., 2014). In the most widely accepted models, eruptions are initiated when pillow lavas are effusively erupted into the meltwater and banked against the steep walls of an englacial lake under high hydrostatic pressure (Guðmundsson, 2005; Jones 1970; Jones 1969; Moore and Calk, 1991; Pollock et al., 2014). As the mound rises, hydrostatic pressure decreases and induces more explosive eruptions (Bennett et al., 2009). The

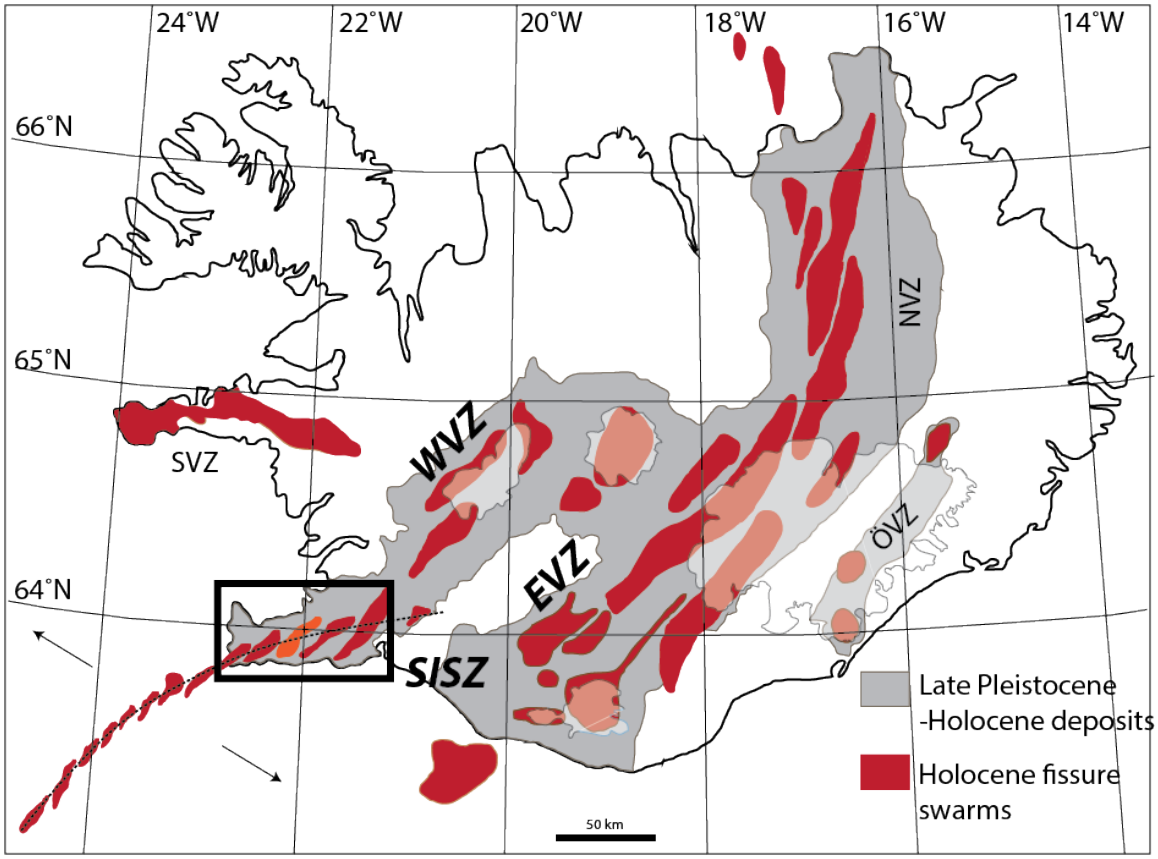

Figure 1. Map of Icelandic volcanism. Reykjanes Peninsula is outlined in the black box, and the spreading ridge regional to the Reykjanes Peninsula is indicated by a dotted line. The Krusivik fissure swarm is highlighted in orange. Adapted from Edwards et al. (2012) and Jakobsson et al. (1977).

explosive eruptions deposit hyaloclastite, breccia, and a tuff cone, which may break through the confining ice (Jones, 1970; Jones 1969; Pollock et al., 2014). If the pile emerges above the ice, it may initiate a subaerial effusive eruption and the formation of a lava cap that creates the flat top of a tuya (Guðmundsson, 2005). The resulting contact with the breccia and lava cap is called the passage zone. Finally, dikes are common and found lava piles (Pollock et al., 2014).

The basaltic Reykjanes Peninsula (Fig. 1) is the subaerial expression of the Mid-Atlantic Ridge in southwest Iceland. It is covered by subglacially erupted tuyas and ridges (tindars) that increase in number to the east (Jakobsson et al., 1977). There has not been glacial cover for 12 to 15 ka, and subaerial Holocene flows filled in the spaces between glaciovolcanic ridges (Jakobsson et al., 1977). The peninsula is the most seismically active part of Iceland and is volcanically active due to a combination of the spreading ridge and mantle plume. A concentration of earthquake epicenters and volcanic activity in a 10 km wide area has been defined as the Reykjanes Volcanic Zone and interpreted as the spreading boundary (Jakobsson et al., 1977; Thordarson and Larsen, 2007). Right stepping en echelon fissure swarms developed along the plate boundary parallel to spreading in the Holocene (Jakobsson et al., 1977). These fissure swarms are expected to exist for 0.5-1.5 Ma (Thordarson and Larsen, 2007).

Field Area

Sveifluhals Ridge is a northeast trending ridge that was erupted subglacially from a fissure about seven km long in what is now the Krusivik fissure system. It was most likely erupted during the Weischellian glaciation, which was the most recent glaciation and spanned from 21 to 10 ka BP (Bourgeois et al., 1998; Pollock et al., 2014). The ridge

is composed of about 150 m of pillow lava, breccia, tuff, and glacial diamict (Pollock et al., 2014).

Undirhlíðar Quarry is a 0.6 km by 0.25 km quarry cut into the northeastern end of Sveifluhals Ridge. Pollock et al. (2014) have defined and mapped the exposed lithologic units as pillow lava, intrusions, tuff-breccia, and lapilli tuff (Fig. 2). Stratigraphically, these form a minimum of eight units that reflect the complexity of the eruption (Pollock et al., 2014). The quarry walls expose thousands of pillow basalts in cross section that were analyzed for this study.

Pillow Lava Morphology

Pillow lavas form a tangled network of subaqueous tubes that are approximately circular or ellipsoidal in cross section (Moore, 1975; Sánchez et al., 2012; Walker, 1992). They are fed from upslope and advance sporadically by exuding bulbous toes of magma in front of one another (Jones, 1968; Macdonald, 1953). It is extremely rare to witness discrete pillow sacks, because pillows are formed at the end of lava tubes. The formation of discrete sacks has only been observed when they break off from the feeding tube and tumble downslope (Jones, 1968; Moore, 1975). Columnar jointed masses observed by Jones (1968) in northeast Iceland were interpreted as pillow lava sources. Massive columnar jointed basalt structures were also found at Undirhlíðar Quarry.

Direct observation by Sánchez et al. (2012) and lab experiments with PEG (polyethylene glycol) by Gregg and Fink (2000) indicate that pillow lavas are emplaced at a relatively low rate (< 1 m^3/s), on low slopes, and with a relatively high cooling rate. Magma moving at a higher velocity would generate sheet flows. It is possible for a lava

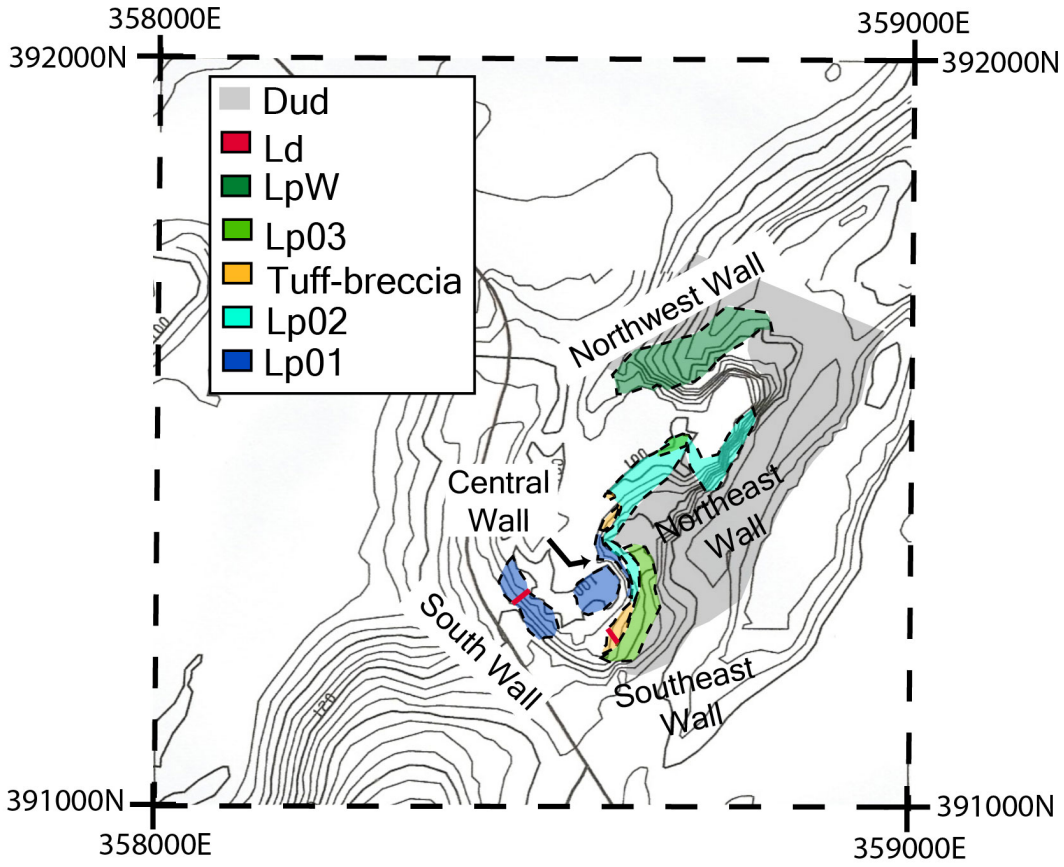

Figure 2. Map of Undirhlíðar Quarry on the northeast end of Sveifluhals Ridge. Quarry walls and lithologic facies are labeled, as defined by Pollock et al. (2014). Pillow units, LpW, Lp01, Lp02, and Lp03, have blue and green fills. Dikes, Ld, are drawn in red. Tuff-breccia is yellow, and Dud is talus and unconsolidated cover. Adapted from Pollock et al. (2014).

flow to start as a sheet flow and slow down to start producing pillows at its toe (Sánchez et al., 2012).

Magma is immediately quenched as it hits the water, forming a bulbous pillow lava with a glassy rind. Sometimes, the glassy rind is corrugated parallel to pillow advancement. However, rinds are not always preserved because the glass is extremely fragile (Moore, 1975; Tepley and Moore, 1974). In the first few seconds after emplacement, gases cool and contract, causing the pillow to implode before continuing to grow (Moore, 1975; Tepley and Moore, 1974). As the pillow loses heat to the water, it cools and forms a crust from the outer edge toward the center. Depending on the thickness of the crust, pillows grow by stretching or by cracking and expanding. Walker (1992) determined that pillow growth is controlled by viscosity, which is in turn controlled by temperature and composition. Smaller pillows grow more rapidly by stretching their skin and, thus, have smooth surfaces, while larger pillows crack and expand parallel to flow (Walker, 1992). Moore (1975) observed that growth was impeded when the crust reached 8 mm, and that it took about 20 minutes for a 5 cm crust to form in a stagnant pillow. Burial by successive pillows and the flow of fresh lava decreases the cooling rate (Gregg and Fink, 2000; Höskuldsson et al., 2006; Moore, 1975). Cracks, however, allow water into the pillow body, causing the pillow to cool more rapidly (Moore, 1975).

Vesicle Distribution

Previous studies of vesicle distribution in pillow lava have identified concentric vesicle patterns, radial pipe vesicles (Sánchez et al., 2012), and distinct vesiculated cores (Höskuldsson et al., 2006). Vesicles have long been recognized as indicators of paleo-

pressures extant during subaqueous lava emplacement (Jones, 1969). Jones (1969) reported vesicle size decrease in pillows at depth. Höskuldsson et al. (2006) have suggested that large vesicle concentrations may record transient pressure changes, such as those caused by sudden drainage events within a subglacial lake. They observed, however, that most pillows less than 0.6 m in diameter lack a vesiculated core. Pipe vesicles may form by rising buoyantly or being pushed inward by the cooling crust of a pillow. The presence of radial pipe vesicles indicates that flow velocity was low enough to prevent them from being sheared away by the flow of lava (Walker, 1992).

Dissolution, expansion, ripening, coalescence, flow, and viscosity control vesicle morphology (Cashman et al., 1994; Gaonac'h et al., 1996; Herd and Pinkerton, 1997; Manga, 1996). Vesicles are usually distributed heterogeneously in lava flows and have variable volumes with ratios between the smallest and largest vesicles up to 10^7 (Gaonac'h et al., 1996). Expansion and diffusion dominate small bubble growth, but coalescence prevails as vesicles increase in size (Gaonac'h et al., 1996). In lava tubes, which may resemble pillow feeding tubes, large vesicles escape via passive rise down tube. Meanwhile, small vesicles develop, indicating continuous volatile exsolution (Cashman et al., 1996).

METHODS

Field work

I made measurements and detailed observations of 47 pillow lavas at the central, opposite-central, south, upper-north, and mid-north walls in Undirhlíðar Quarry. I developed a system to categorize pillow vesicle patterns into six types based on the presence of a vesiculated core, vesicles in the body, and a hollow pocket (Fig. 3). Cores

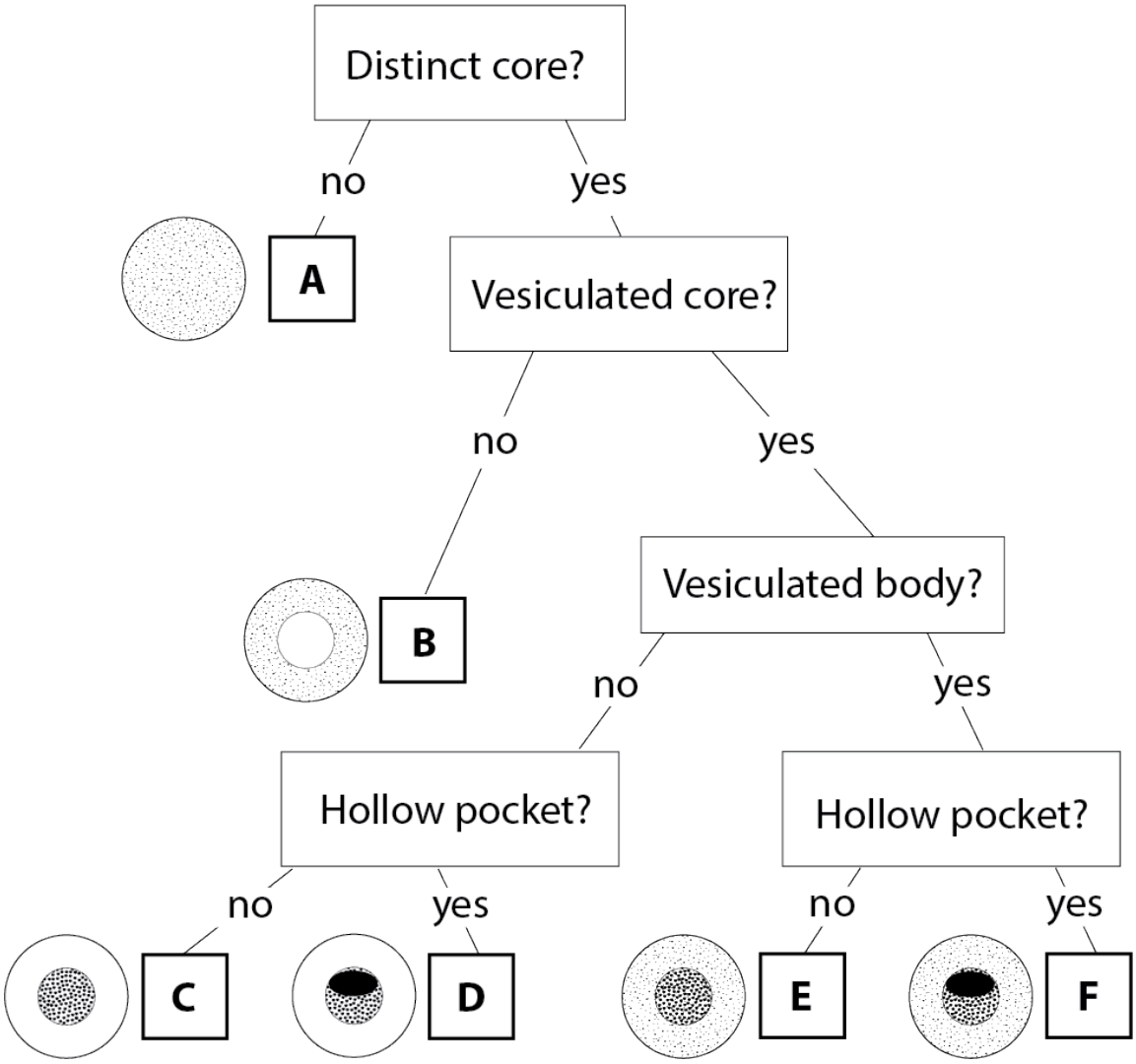

Figure 3. Flow chart used to assign vesicle distribution type to pillow cross sections. A distinct core was defined as a core with vesicles of notably different size and/or concentration than vesicles in the body. A vesiculated core was defined as a core with vesicles significantly larger and/or more concentrated than vesicles in the pillow body. The pillow body was defined as the area of the pillow outside its core. A vesiculated body referred to a pillow body with vesicles visible to the naked eye. Some pillow bodies were not considered vesiculated if they only contained a few visible vesicles. Finally, a hollow pocket was defined as a cavity in a pillow core that was larger than a vesicle or fracture. If pillows have concentric vesicle rings, it was denoted with an r.

are distinguished by a different concentration and/or average size of vesicles from the pillow body.

Type A pillows have no core and no hollow pocket. Type B pillows have a vesiculated body and a core with no or very few vesicles. Type C pillows have a non-vesiculated body and a vesiculated core. Type D pillows have a non-vesiculated body and a vesiculated core with a hollow pocket. Type E pillows have a vesiculated body and a vesiculated core. Type F pillows have a vesiculated body and a vesiculated core with a hollow pocket. If a pillow has vesicle rings, it is denoted with an r after the letter. Figure 4 gives an example of every observed pillow type with and without vesicle rings.

I further categorized pillows based on the presence of concentric vesicle rings on a scale from zero (no rings) to three (well-defined rings) (Fig. 5). Instead using random sampling, I recorded pillows in an attempt to account for every recognizable type on all five quarry walls. I also recorded pillow dimensions and locations, made sketches, took high resolution photographs, and collected hand samples that included glass rims, pipe vesicles, a densely vesiculated core, and a pillow section that spanned the edge to the center.

Image Processing

Using Adobe Illustrator, I traced vesicles from the photograph of a type Ar pillow in transects radiating from the pillow center to the edge (Fig. 6). Trace P11UN01 is a vertical transect from the center to the top of the pillow, and P11UN02 is a transect from the center to the right side. The pillow, numbered P11UN, is found at coordinates 391788.894N, 358878.92E, 160.06 msl, zone 27W, on the upper-northwest wall of the quarry. Image resolution limited minimum traceable vesicle size. By this method, I

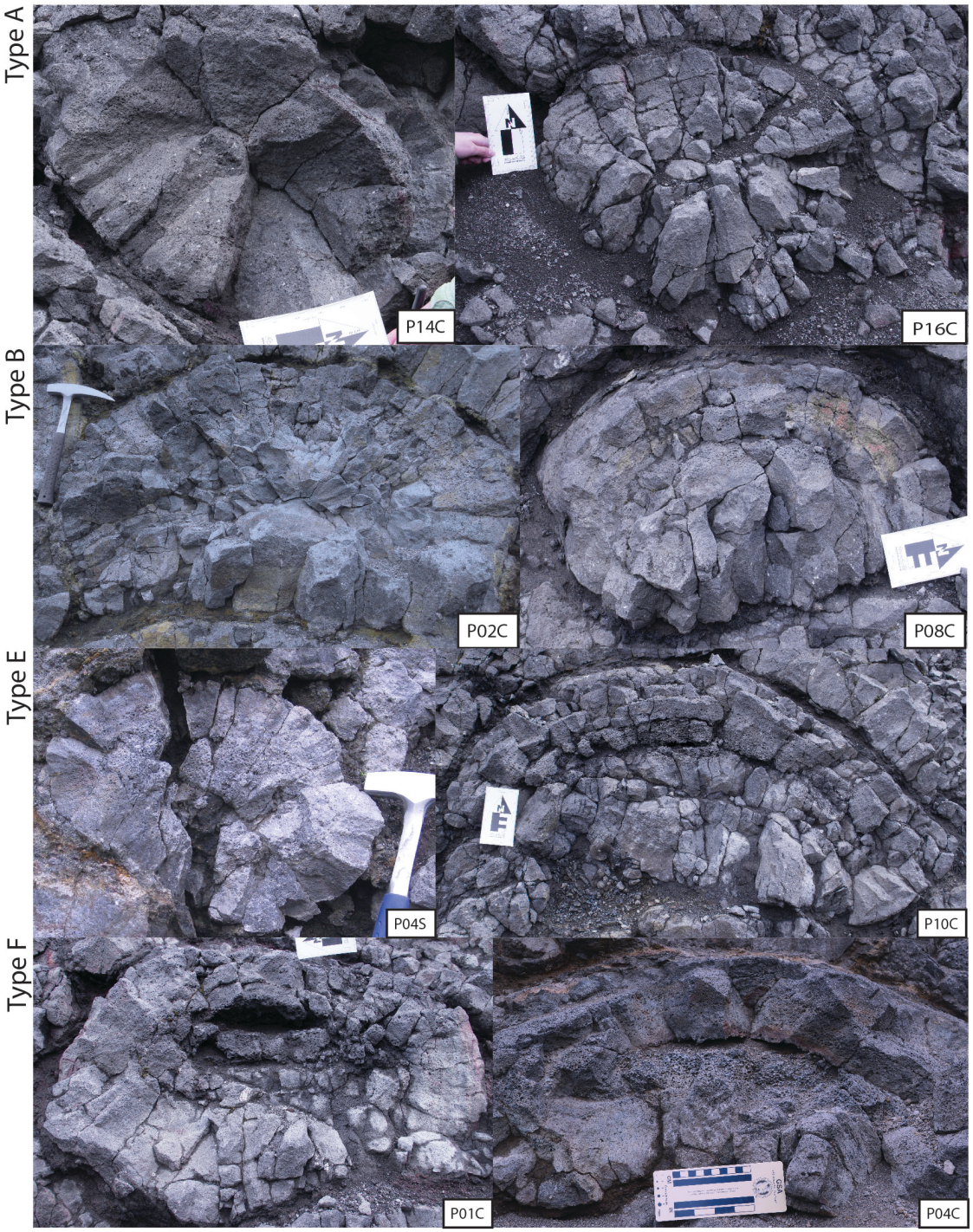

Figure 4. Example pillows of each type found in Undirhlíðar Quarry. The hypothetical types C and D were not observed or photographed. Types B and F were only found with vesicle rings. Types A and B are shown without (left) and with (right) vesicle rings.

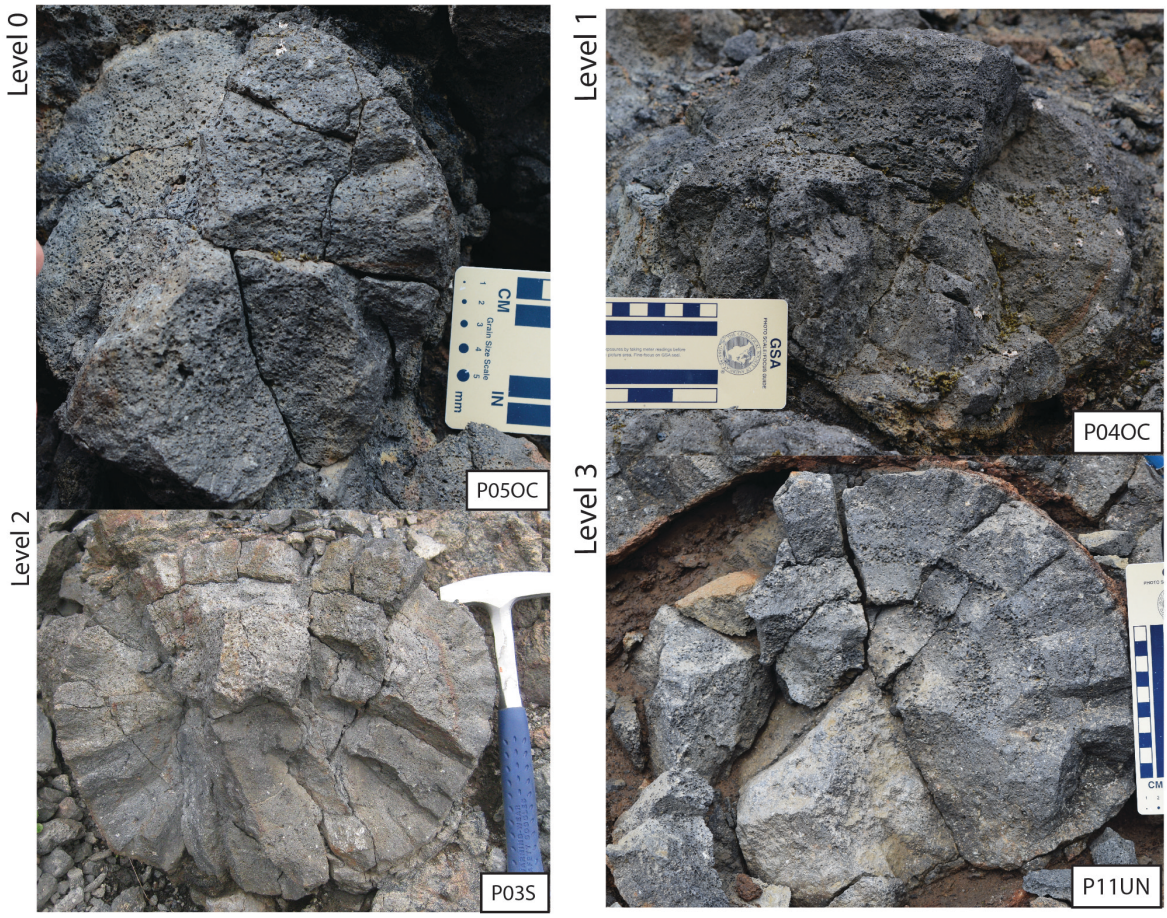

Figure 5. Examples of the different levels of vesicle rings in type A pillows found in Undirhlíðar Quarry. Rings are also commonly found in all other pillow types.

Figure 6. Vesicle trace of two transects of pillow P11UN. Trace P11UN01 is vertical, and P11UN02 is horizontal. Traces were made on the most visible portions of the pillow, where the most complete transects was could be made without crossing fractures or other obstacles.

produced images of planar cuts through vesicles, which I imported into ImageJ in 0.5 cm segments to analyze vesicle size, percent area vesiculated, density, aspect ratio, and circularity. I analyzed vesicle traces in 0.5 cm thick segments from core to edge.

Vesicles closest to the edge of the pillow were quenched most quickly and, thus, provide the closest estimate to initial vesicle size. Low points in vesicle circularity or aspect ratio could indicate deformation by flow, hitting a barrier, or coalescence. Coalescence also forms larger vesicles. Both of these pillows are in the top half of the pillow where vesicles collect and are most likely to coalesce. Alternatively, large or dense vesicles could indicate a change in pressure.

Hand Samples

Sample 16AT01 spanned pillow P11UN from center to edge. It was divided into three sections (A, B, and C) where it broke along well-defined vesicle rings. To look for compositional variations within the pillow, I prepared glass beads from fresh whole-rock powder closest to the core (A), center (B), and edge (C). They were analyzed by XRF at the College of Wooster for major element geochemistry. XRF sample preparation and analysis followed the methods of Pollock et al. (2014).

I had thin sections prepared from sample 16AT01 A, B, and C that spanned pillow P11UN from the core to the edge. To fit the entire transect on slides, I divided 16AT01C into 16AT01C and 16AT01D.

I analyzed plagioclase crystal size and chemistry across the pillow transect, using Carleton College's Hitachi S-3000N Scanning Electron Microscope (SEM) equipped with an Oxford INCA microanalysis system. I operated the SEM with a voltage of 20 kV, beam current between 95 and 106 uA, and working distance of 15 mm. To avoid

charging, I operated the SEM in variable pressure mode at 20 Pa. I analyzed mineral chemistry at 1000x magnification at five sites of interest on both ends of each thin section, which were proximal to the vesicle rings. At each site of interest, I measured mineral composition on three plagioclase crystals (microlites). When possible, I took measurements adjacent to crystal rims to avoid zoning variations, however crystals were small enough that measurements usually had to be taken at the center. I captured images at 120x magnification in these areas to compare crystal size.

Vertical Distribution Model

I created a one-dimensional model to calculate the vertical distribution of a stagnant pillow lava. The inputs to the model are pillow radius, vesicle radius, pressure, temperature throughout the pillow, and the temperature cutoff (the temperature at which vesicles can no longer move through the melt). The model breaks a vertical pillow transect into 20 stacked blocks that each have a unique temperature, viscosity, and terminal rise velocity. The simulation begins with 21 equally spaced vesicles that are allowed to rise over time following the constraints of the model.

Temperature

I assumed the initial emplacement temperature across the pillow was the liquidus temperature. The MELTS applet, based upon the work of Ghiorso and Sack (1995) and Asimow and Ghiorso (1998), was able to determine the liquidus temperature from major element composition. I input the major element composition of sample 16AT01A at an oxygen fugacity set to the QFM+ buffer and a pressure of 2000 bars (assuming the source magma chamber was at a depth of ~6.7 km) to calculate the liquidus at 1216 °C. A pillow

cooling model written by Ben Edwards, using equations from Crank (1975) for diffusion in a cylinder and Bessel Functions, defines temperature in the following time steps.

Viscosity

At each time step, the model calculates the viscosity of every block using the methods of Giordano et al. (2008), which input the major element geochemistry of sample 16AT01A and temperature. In an alternative version, it calculates viscosity using MELTS from the major element geochemistry of sample 16AT01A, temperature, and pressure (Asimow and Ghiorso, 1998; Ghiorso and Sack, 1995). According to Marsh (1995), vesicles can no longer move through a magma made up of more than 55 % crystals. Thus, the temperature cutoff for the model is considered the temperature at which magma crystallinity reaches 55 %. I determined this temperature by using MELTS to identify the viscosity at which the liquid mass reaches 55 %.

Terminal Rise Velocity

The model calculates the terminal rise velocity of vesicles in each block using Stoke's Law, which inputs vesicle size, the density of a vesicle, magma density, and magma viscosity. The vesicle size used is the average size of the vesicles traced for image analysis on pillow P11UN, based on ImageJ results. Vesicle density is that of air, 1 kg/m^3. The model determines magma density from major element geochemistry, pressure, and temperature of the block, using the methods of Bottinga and Weill (1970). Fresh glass collected from the same outcrop and at a similar elevation to sample 16AT01A provided the pressure value. A fellow Keck student, Chloe Wallace, used a solubility model to calculate an eruption pressure of 5 bars for the glass that corresponds

to an ice thickness of 55.64 m. In the model, Wallace input composition; water content, calculated using FTIR; and the liquidus temperature, determined by MELTS.

Vesicle Rise

The model uses the terminal rise velocity and assigned time step to calculate vesicle rise in each block. If the amount of rise takes the vesicle into the above block, the additional rise is calculated with regards to the viscosity of the new block. If a vesicle reaches a block less than or equal to the temperature cutoff or the top edge of the pillow, it will not rise beyond that boundary.

RESULTS

Pillow-Scale Observations

Every observed pillow in Undirhlíðar Quarry contains at least some vesicles. They range in size from microscopic to centimeter scale. Large vesicles are consistently found concentrated in glass rims, where they were quenched almost immediately upon contact with ice.

I observed two trends in vesicle distribution. First, vesicles concentrate in the upper half of pillows, where, in some cases, there is also a hollow pocket (Fig. 4, type F). Second, vesicles are typically distributed concentrically in the form of rings or distinct cores (Fig. 5). The largest and most highly concentrated vesicles are found in the upper half of the core or vesicle rings. In some less common cases, pillows have dense cores with very small or no vesicles (Fig. 4, type B).

I identified four out of six possible vesicle distribution types. I did not observe pillow types C or D anywhere in the quarry. While some pillows have non-vesiculated cores (type B), all observed pillows have vesiculated bodies.

I recorded the pillow types present on each quarry wall (Fig. 7). Pillows without a defined core (type A) were observed at all the walls. Pillows with vesiculated cores (type E) were identified at all the walls except the mid-north wall. The mid-north wall was not recorded completely, however, so the possible presence of type E pillows should not be discounted. The less common types were pillows with hollow pockets (type F), unique to the central wall, and pillows with non-vesiculated cores (type B), which were unique to the central and upper-north walls.

I plotted pillow size and aspect ratios in Figures 8 and 9, respectively. These plots reveal that type B pillows are the largest. On average, their area is nearly twice that of the other pillow types (Fig. 8). Type A pillows, which do not have distinct cores, are the most circular, and type F, which have hollow pockets, are the least (Fig. 9). A plot of aspect ratio vs. area (Fig. 10) reveals that they are loosely correlated.

Figure 11 shows the relationship between ring level and pillow type. Note that type B pillows always have vesicle rings and have the most well defined rings (a combination of ranking 2 and 3).

ImageJ Analysis

I plotted the results of the ImageJ analyses to determine what vesicle characteristics define vesicle rings (Fig. 12). There are noticeable peaks in the plots of average vesicle size and percent area vesiculated that correspond with the position of vesicle rings in both transects from pillow P11UN. There is a slight peak in average aspect ratio and a low point in average circularity corresponding to the position of vesicle rings in trace P11UN02. However these peaks are not distinct enough to be confidently attributed to the presence of vesicle rings. There are no distinguishable peaks or low

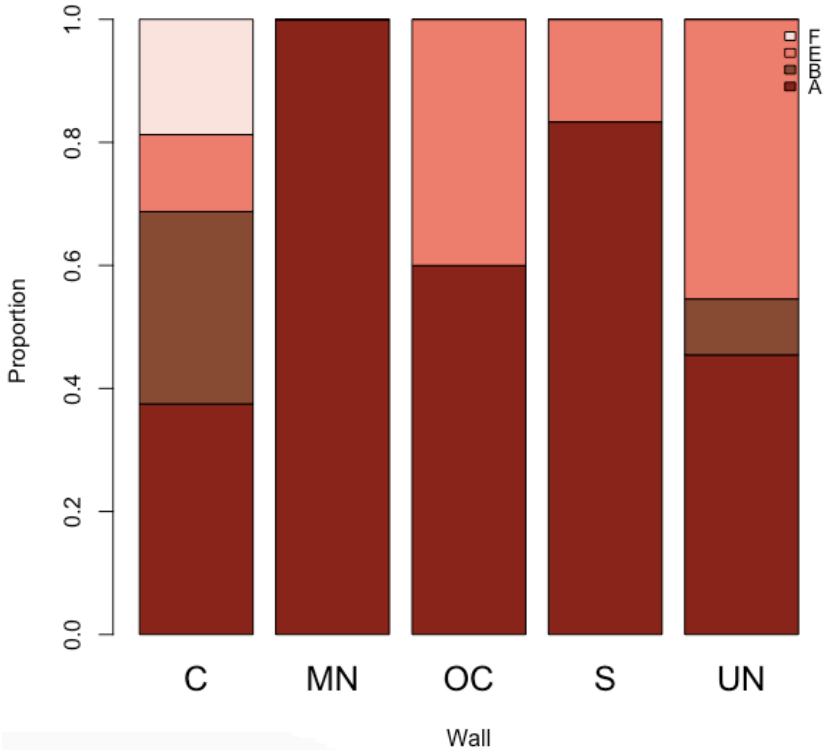

Figure 7. Proportion of each pillow type found in quarry walls. Wall names are abbreviated as central (C), mid-north (MN), opposite-central (OC), south (S), and upper-north (UN).

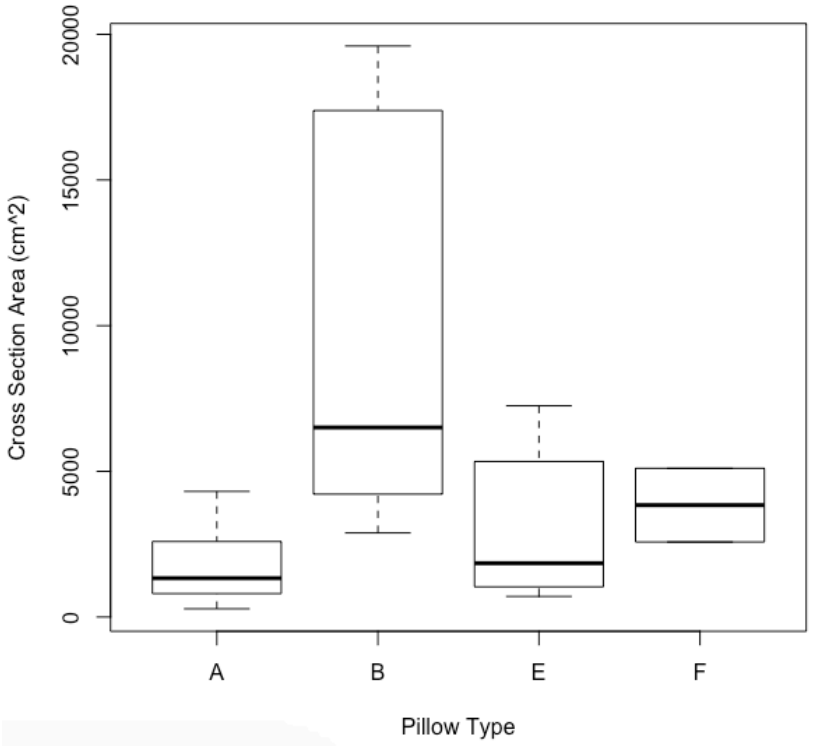

Figure 8. Approximate cross-sectional area by pillow type. Area is calculated assuming pillows are perfect upright ellipses.

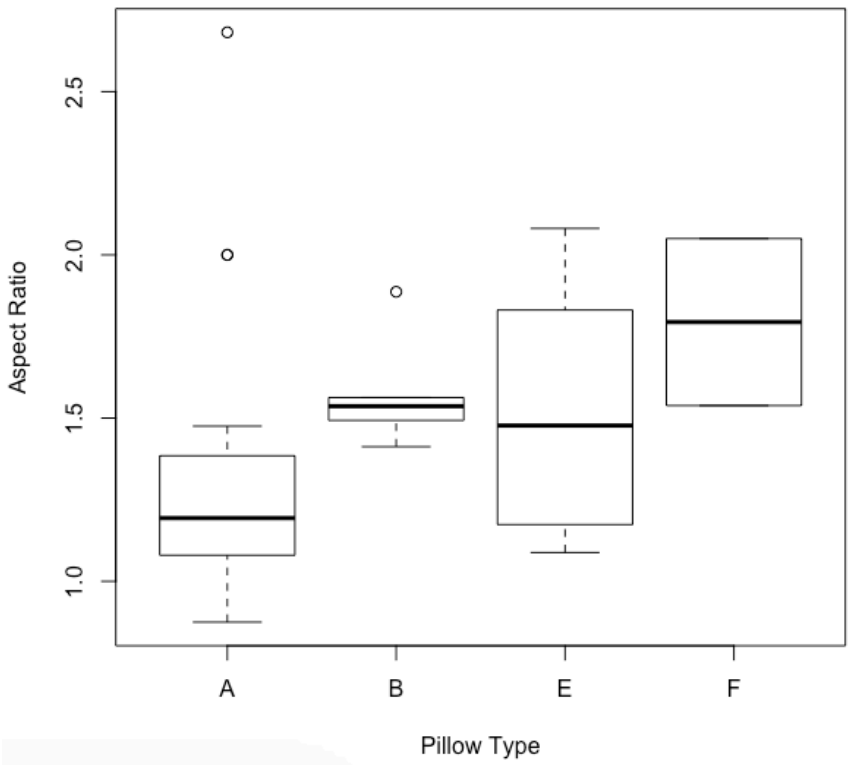

Figure 9. Aspect ratio (width/height) by pillow type.

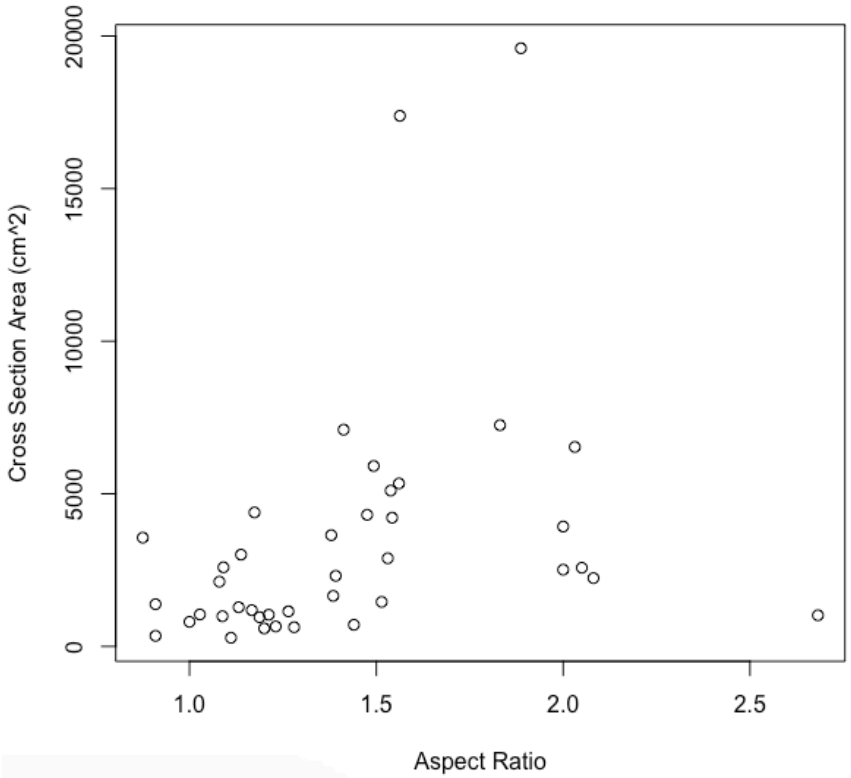

Figure 10. Plot of the cross-sectional area vs. aspect ratio of measured pillows in Undirhlíðar Quarry. They are very loosely correlated.

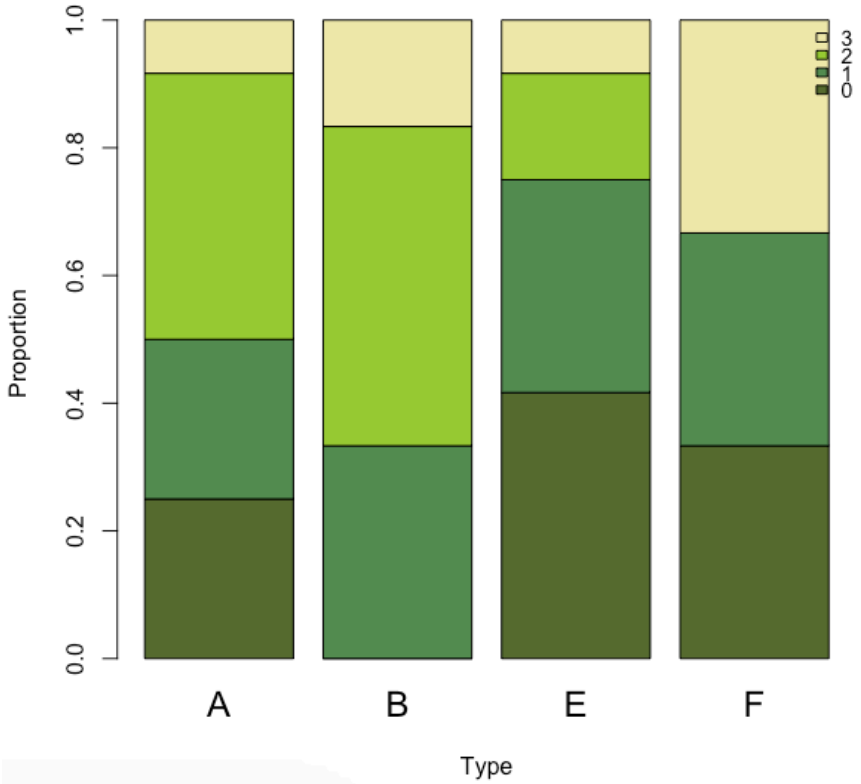

Figure 11. Levels of vesiculated rings in each pillow type from 0 (no rings) to 3 (well-defined rings).

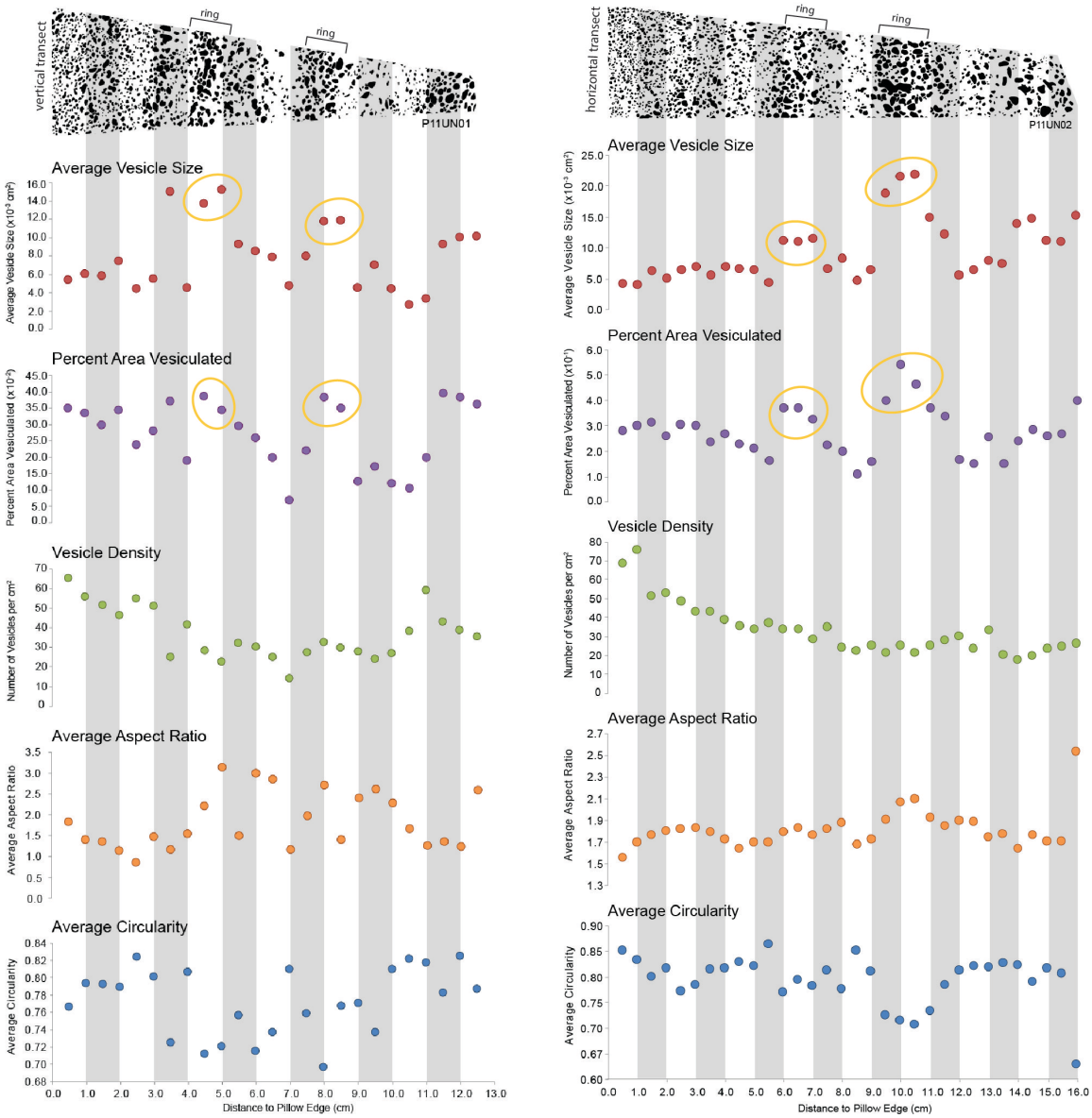

Figure 12. Values from ImageJ analysis of trace P11UN01 and P11UN02 in 1/2 cm segments identified by gray and white bars. Peaks that correspond with vesicle rings are circled.

points that correspond with the vesicle rings in trace P11UN01. There is no distinguishable peak or low point on the vesicle density plot, so it is not considered to be related to the presence of vesicle rings.

The shape of some of the larger vesicles makes it clear that there has been coalescence where the inner wall has not fully retracted. It is not obvious, however, whether this is the primary mechanism of vesicle growth in this pillow.

Geochemistry and Thin Sections

XRF geochemistry results of 16AT01A, 16AT01B, and 16AT01C from pillow P11UN (Fig. 13) indicate that vesicle patterns are not compositionally controlled, because the major element concentrations are very similar across the pillow (Table 1) and all plot as basalt on a TAS diagram (Fig. 15).

Albite content ranged from Ab_{29} to Ab_{36} (Table 2) and crystal size results varied, but revealed no regular pattern relevant to vesicle rings along the transect (Fig. 14). Fe content was unusually high for plagioclase crystals.

Vertical Distribution Model

The results of the vertical distribution model for a 0.5 m-, 1.0 m-, and 1.5 m-diameter pillow (Fig. 16) demonstrate how most vesicles concentrate in the top halves of pillows, while a few are trapped by viscous lava and remain in the lower halves. At time zero, vesicles are distributed evenly. Over time, vesicles rise, and the pillow cools from above and below. The vesicles rise more slowly on the edges where the pillow is cooling and more viscous. They are unable to move or pool against cooling fronts where the melt becomes too viscous at 55 % or more crystallinity. For example, it is possible to see where three vesicles pool against a cooling front at 1.25 m between 2.0 to 2.5 h of

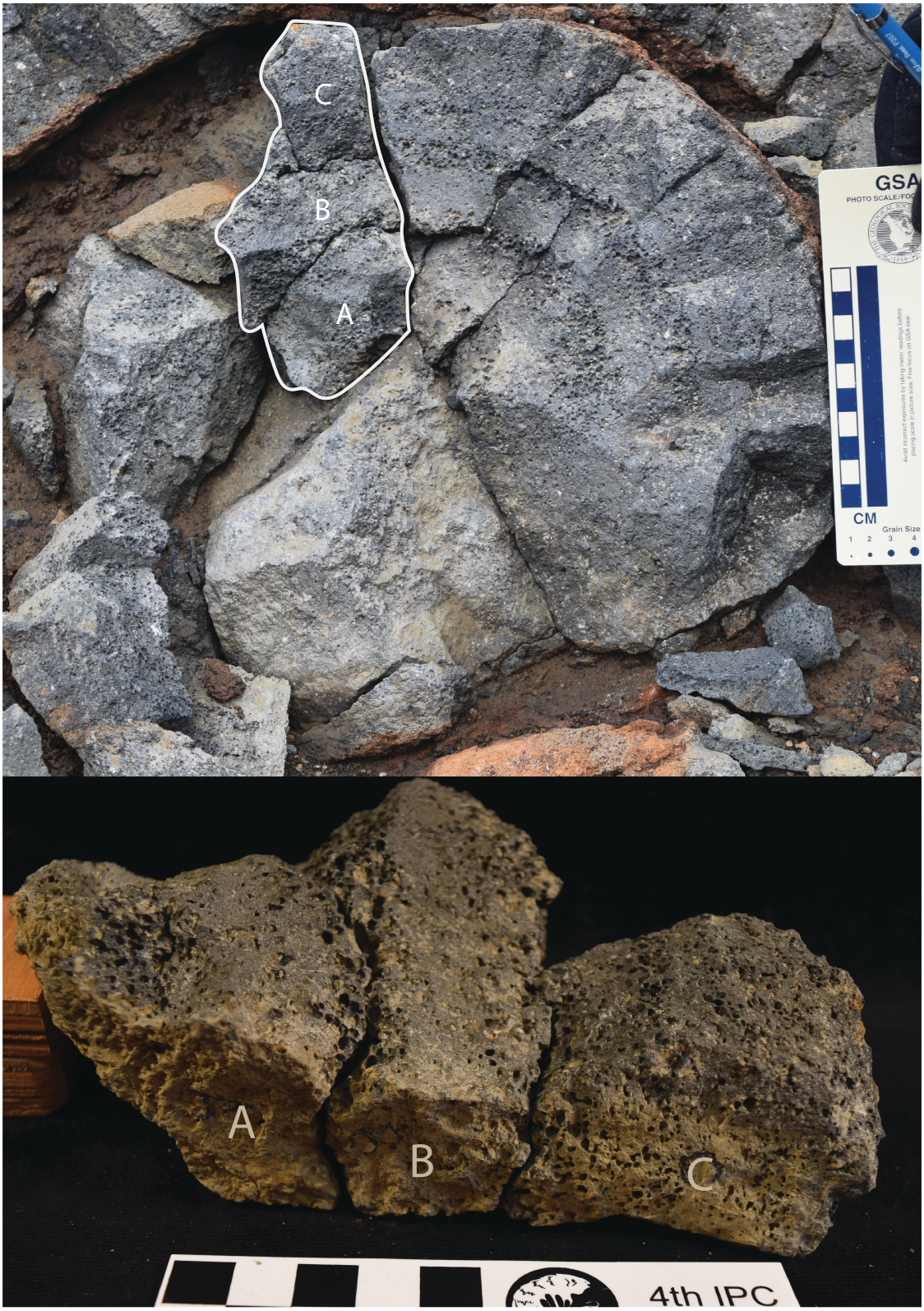

Figure 13. Sample 16AT01 A, B, and C, collected from pillow P11UN. Major element geochemistry was analyzed for the innermost portion of A, the center of B, and the outermost portion of C.

Table 1. Major element geochemistry of 16AT01

	16AT01A	16AT01B	16AT01C
Major Elements (wt.%)			
SiO2	48.13	48.13	48.13
TiO2	1.74	1.69	1.63
Al2O3	15.80	16.05	16.28
FeO*	11.86	11.60	11.31
MnO	0.20	0.19	0.19
MgO	7.77	7.85	8.02
CaO	11.97	11.95	11.92
Na2O	2.23	2.25	2.22
K2O	0.14	0.14	0.14
P2O5	0.15	0.15	0.15
Sum	100.00	100.00	100.00

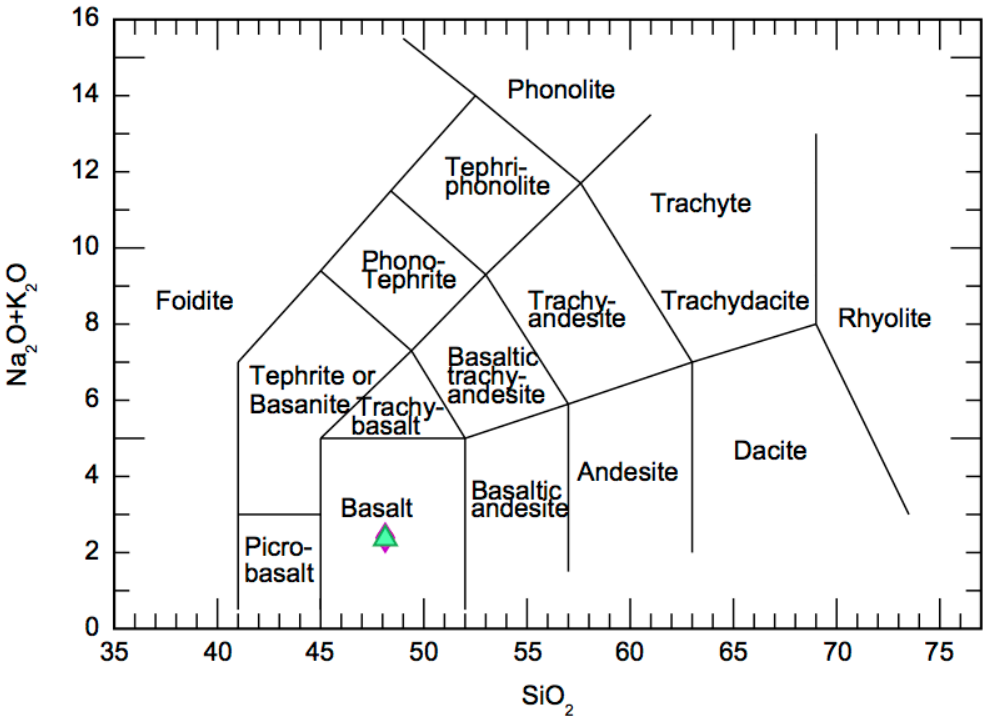

Figure 15. Bulk composition of samples 16AT01A, 16AT01B, and 16AT01C plotted on the total alkali-silica diagram by LeBas et al. (1986). All samples plot as basalt.

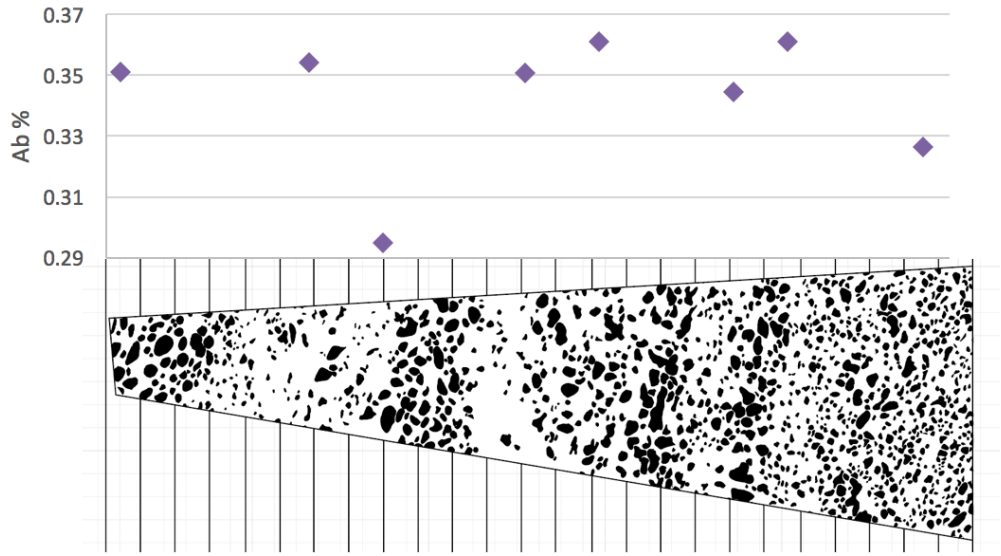

Figure 14. Albite content of plagioclase crystals in different positions throughout sample 16AT01. Variations are not relevant to ring position.

Table 2. Average mineral analyses for plagioclase crystals in 16AT01

	a1	a2	a3	a4	a5	a6	a7
SiO2	53.33	53.28	50.97	53.82	53.52	53.21	53.96
Al2O3	27.29	27.40	16.79	26.75	26.19	26.04	26.31
TiO2	0.00	0.00	0.80	0.07	0.05	0.26	0.05
FeO	2.83	2.63	10.40	2.83	3.07	3.20	2.94
MgO	0.87	1.00	7.65	0.94	1.22	1.28	1.30
MnO	0.00	0.00	0.00	0.00	0.00	0.00	0.00
CaO	12.08	12.04	10.77	12.01	12.16	12.41	11.76
K2O	0.00	0.00	0.10	0.00	0.00	0.00	0.00
Na2O	3.61	3.65	2.52	3.59	3.80	3.61	3.67
total:	100.00	100.00	100.00	100.00	100.00	100.00	100.00
Basis:	8 Ox	8 Ox	8 Ox	8 Ox	8 Ox	8 Ox	8 Ox
Si	2.44	2.43	2.44	2.46	2.45	2.44	2.47
Al	1.47	1.48	0.95	1.44	1.42	1.41	1.42
Ti	0.00	0.00	0.03	0.00	0.00	0.01	0.00
Fe2+	0.11	0.10	0.42	0.11	0.12	0.12	0.11
Mg	0.06	0.07	0.55	0.06	0.08	0.09	0.09
Mn	0.00	0.00	0.00	0.00	0.00	0.00	0.00
Ca	0.59	0.59	0.55	0.59	0.60	0.61	0.58
K	0.00	0.00	0.01	0.00	0.00	0.00	0.00
Na	0.32	0.32	0.23	0.32	0.34	0.32	0.33
cations:	4.99	4.99	5.18	4.98	5.01	5.00	4.99
XCa	0.65	0.65	0.70	0.65	0.64	0.66	0.64
XK	0.00	0.00	0.01	0.00	0.00	0.00	0.00
XNa	0.35	0.35	0.29	0.35	0.36	0.34	0.36

note: Site a1 is closest to the core, and site a7 is closest to the edge.

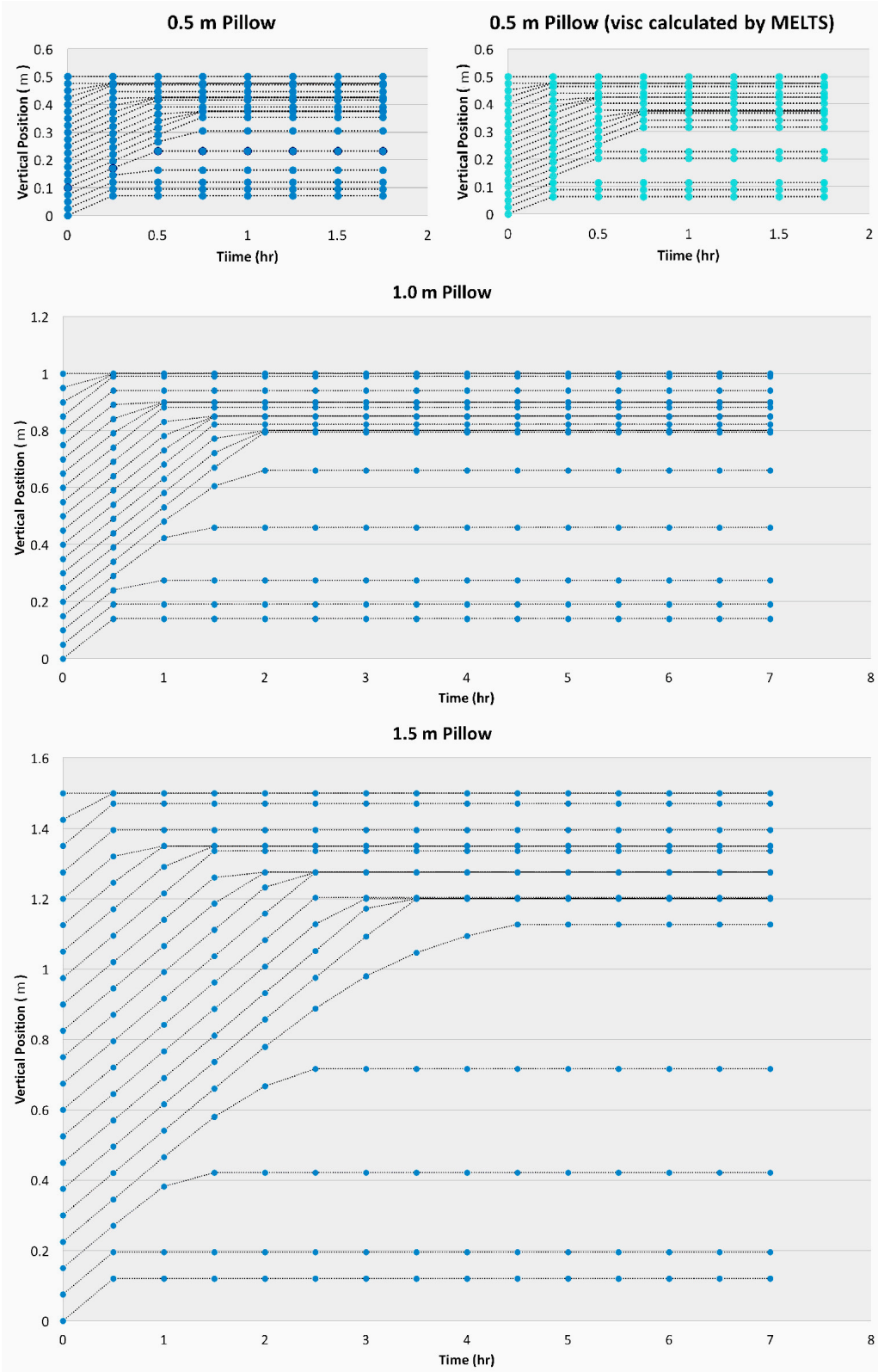

Figure 16. Results of the vertical distribution model with variable pillow diameters and viscosity calculation methods. Note the different x-axis scale for 0.5 m pillows.

cooling in a 1.5 m pillow.

The comparison of the three plots of differently sized pillows shows that vesicles are most evenly distributed in smaller pillows by the time they cool. A 0.5 m diameter pillow reaches 55% crystallinity in 0.75 h. Conversely, the vesicles of a 1.5 m pillow are more concentrated at the top. They have 4.5 h to rise before the entire pillow has reached at least 55% crystallinity.

The plots of vesicle position in a 0.5 m pillow calculated with MELTS viscosity methods (bright blue) versus Giordano et al. (2008) viscosity methods (dark blue) are compared side by side (Fig. 16). Because the MELTS model calculates slightly higher viscosities than Giordano et al. (2008) for each temperature, more vesicles were trapped at the bottom edge, and others did not rise as far.

DISCUSSION

Interpretation of Pillow Types

Höskuldsson et al. (2006) observed that small pillows are relatively round and lack a vesiculated core. Type A pillows, which are the smallest of the observed types, also have these characteristics. Because of their size and shape, they probably grow by stretching (Walker, 1992). I propose that type A pillows are the farthest-reaching extent of pillow tubes, thus being smaller than their upslope counterparts. At the end of a tube, a pillow would be emplaced at a lower temperature and have more contact with the water. As a result, the pillow would cool more quickly, leaving less time for vesicles to rise. This is consistent with the observation that vesicles in type A pillows are relatively evenly dispersed.

Type B pillows are the largest type on average, indicating that they grew for a longer period of time. Type B pillows were most likely emplaced near the source as feeder tubes and cooled slowly because of the flow of lava through their center. Type B pillow cores are distinct because they contain few vesicles, if any. Being near the source, they would not have solidified before a later eruption filled the distinctly non-vesiculated cores with degassed magma containing few vesicles. In support of this explanation, the massive columnar jointed basalt in Undirhlíðar Quarry, which was identified as a possible source to the pillows, also had very few vesicles.

Type E pillows are characterized by their highly vesiculated cores. Höskuldsson et al. (2006) proposed that vesiculated cores are a result of extreme changes in pressure. The proposed source of the pressure change are major glacial flood events called jökulhlaups that rapidly drain englacial lakes. Sudden depressurization could reactivate the eruption, which would result in new pulses of magma and larger vesicles (Höskuldsson et al., 2006). In conjunction with Stoke's Law, the thickness of the pillow body between the edge and the core can be used to estimate the minimum amount of time that followed the initial placement of the lava and the following jökulhlaup.

The source of type F pillows was probably cut off or diverted, distinguishing these pillows from type B and E pillows. A hollow pocket may have formed in the wake of the still liquid lava that drained the tube (Moore, 1975). The flattened shape of type F pillows indicates that the pillows were soft when they were drained, causing them to slump as they cooled with no support from their hollow centers. Moore and Schilling (1972) pulled up dredges from the Reykjanes Ridge with many pieces of hollow pillow, indicating that type F pillows are common in other parts of Iceland.

Vesicle Rings

Concentric vesicle rings are a prominent feature in all pillow types at Undirhlíðar Quarry. ImageJ results revealed that they are defined by size and density. The increase in size and density could be a result of either coalescence or a pressure change.

Flow through pillow tubes may organize vesicles in cylinders similar to the way they form sheets in lava flows (Manga, 1996) (Fig. 17). If this were the case, the pillow would have to cool rapidly after emplacement before the vesicles rise out of their concentric position. This explanation does not account for pillow formation without rings or the fact that type B pillows always have rings, despite being large and presumably slow cooling.

Another possible interpretation is that each vesicle ring represents a pulse of fresh magma (Fig. 17). At t_0, a new pillow tube is emplaced with evenly distributed vesicles. A glassy rim is immediately quenched. At t_1, vesicles move to the edge of the pillow. By t_2, a few centimeters of crust have cooled, trapping the highest concentration of vesicles where they have pooled on the outside edge. At t_3, a new pulse of magma is fed through the tube. Vesicles pool against the new cooling front in t_4. The cooling front continues to move inward, locking vesicles from the second pulse in place in t_5. This process can be repeated as many times as necessary to match the observed number of rings. The inward growth also accommodates the formation of a different type of core, like those observed in pillow types B and F.

Vertical Distribution Model

Vesicles are most evenly distributed in smaller pillows because the cutoff temperature reaches the center more quickly in a small pillow. Conversely, the vesicles of a 1.5 m pillow are more concentrated at the top because fewer vesicles are caught by the

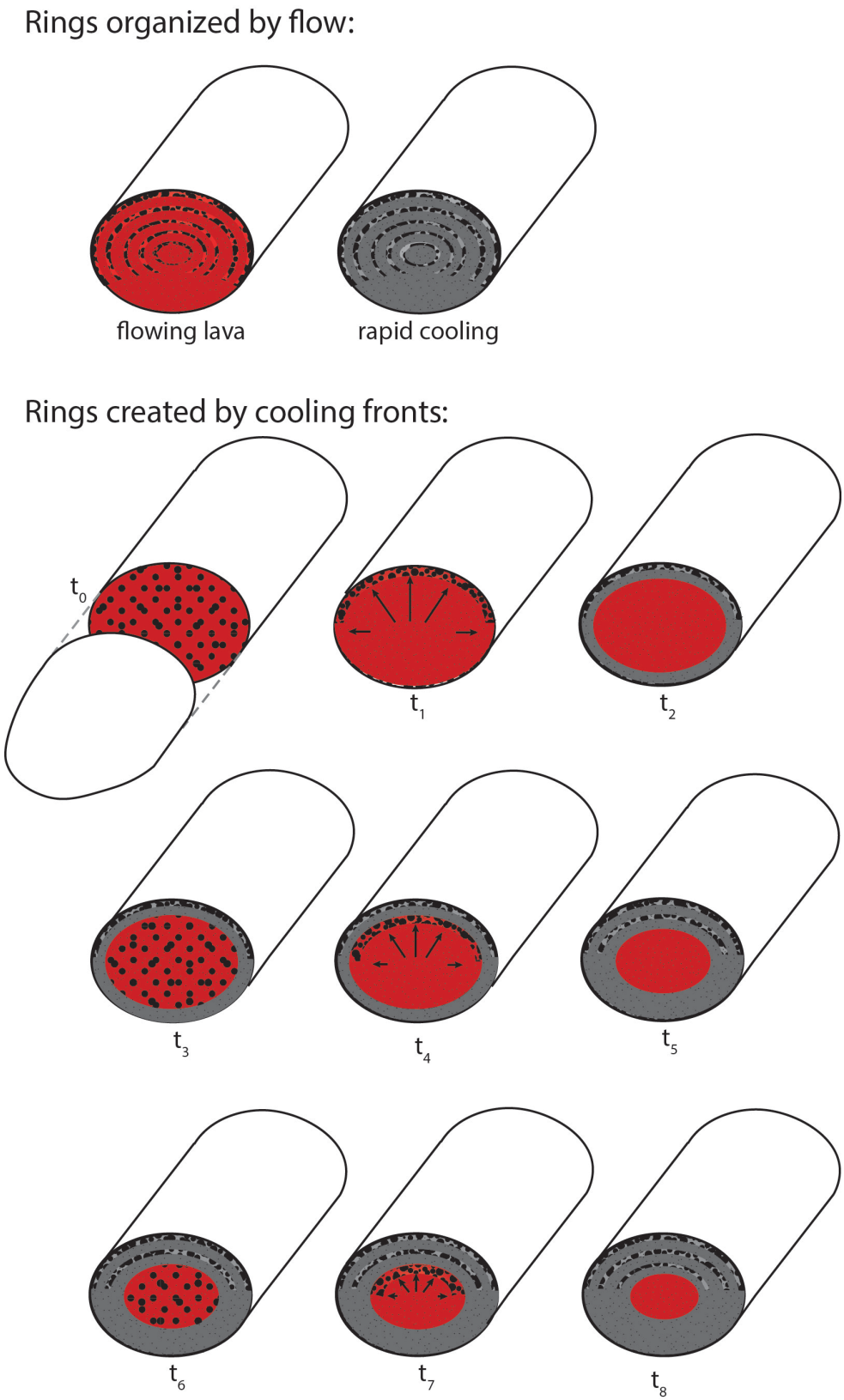

Figure 17. Two possible mechanisms for vesicle ring formation. Rings are more concentrated in the upper half than the lower half of pillows.

cooling front on the bottom edge.

The proposed setting of type A pillows could be modeled using the vertical distribution model. The observed distribution most closely matches the results that the simulation produced for small pillows like type A. I was able to model how vesicles collect at the pillow edge, and could make further adjustments to simulate the possible formation of rings with new pulses of magma and vesicles that pool against cooled margins.

This model is limited because it only accounts for vesicle rise due to gravity and viscosity while the pillow cools and assumes that vesicle position is homogenous at emplacement. It further assumes that the pillow edge is in constant contact with zero degree water and that the lava is stagnant and cools only by conduction.

CONCLUSIONS

My goal was to understand what controls vesicle distribution, and to develop a method to infer eruption environment based on recognizable vesicle patterns. My investigation revealed that vesicle distribution is controlled by gravity, viscosity, and pressure but is not influenced by magma composition. An increase in vesicle size and number characterizes vesicle rings and cores. Rings and cores may represent different events, like magma pulses or sudden changes of pressure in the surrounding environment. The type of vesicle distribution in a pillow cross section may be used to infer proximity to the source, the rate at which the pillow cooled, and eruption events during pillow emplacement. Future studies that systematically characterize the distribution of pillow types at different elevations or distances from the source could be used to support these findings.

ACKNOWLEDGEMENTS

I would like to thank my advisors Meagen Pollock and Ben Edwards for their guidance in the development and completion of this project. Thank you also to Cam Davidson for his guidance at Carleton and help with the SEM. This project was made possible with funding from the Keck Geology Consortium, the National Science Foundation (NSF-REU1358987), and ExxonMobil Corporation. The Carleton College Geology Department provided funding that allowed me to attend and present this research at the GSA annual meeting in 2016. Finally, a huge thanks goes out to Michelle Orden, Chloe Wallace, Rachel Heineman, Cara Lembo, Carl-Lars Engen, Ben Kumpf, and Will Kochtitzky for assistance in the field and moral support.

REFERENCES

Allen, C.C., 1979, Volcaono-ice interactions on Mars: Journal of Geophysical Research, v. 84, p. 8048-8059, doi: 10.1029/JB084iB14p08048.

Asimow, P.D., and Ghiorso, M.S., 1998, Algorithmic modifications extending MELTS to calculate subsolidus phase relations: American Mineralogist, v. 83, p. 1127-1131.

Bennett, M.R., Huddart, D., and Gonzales, S., 2009. Glaciovolcanic landsystems and large-scale glaciotectonic deformation along the Brekknafjöll-Jarlhettur, Iceland: Quaternary Science Reviews, v. 28, p. 647-676, doi: 10.1016/j.quascirev.2008.07.018.

Bottinga, Y., and Weill, D.F., 1970, Densities of liquid silicate systems calculated from partial molar volumes of oxide components: American Journal of Science, v. 269, p. 169-182.

Bourgeois, O., Dauteuil, O., and Van Vliet-Lanoë, B., 1998, Pleistocene subglacial volcanism in Iceland: Tectonic implications: Earth and Planetary Science Letters, v. 164, p. 165-178.

Cashman, K.V., Mangan, M.T., and Newman, S., Surface degassing and modifications to vesicle size distributions in active basalt flows: Journal of Volcanology and Geothermal Research, v. 61, p. 45-68.

Crank, J., 1975, Diffusion in a Cylinder, *in* The mathematics of diffusion: Oxford, Clarendon Press (second edition), p. 69-88.

Edwards, B.R., Magnusson, E., Thordarson, T., Guðmundsson, M.T., Höskuldsson, A., Oddson, B., and Haklar, J., 2012, Interactions between lava and snow/ice during the 2010 Fimmvörðuháls eruption, south-central Iceland: Journal of Geophysical Research, v. 117, doi: 10.1029/2011JB008985.

Gaonac'h, H., Lovejoy, S., Stix, J., and Scherzter, D., 1996, A scaling growth model for bubbles in basaltic lava flows: Earth and Planetary Science Letters, v. 139, p. 395-409.

Ghiorso, M.S., and Sack, R.O., 1995, Chemical mass transfer in magmatic processes. IV. A revised and internally consistent thermodynamic model for the interpolation and extrapolation of liquid-solid equilibria in magmatic systems at elevated temperatures and pressures: Contributions to Mineralogy and Petrology, v. 119, p. 197-212.

Giordano, D., Russell, J.K., and Dingwell, D.B., 2008, Viscosity of magmatic liquids: A model: Earth and Planetary Science Letters, v. 271, p. 123-134. doi:10.1016/j.epsl.2008.03.038

Gregg, T.K.P., and Fink, J.H., 2000, A laboratory investigation into the effects of slope on lava flow morphology: Journal of Volcanology and Geothermal Research, v. 96, p. 145-159.

Guðmundsson, M.T., 2005, Subglacial volcanic activity in Iceland *in* Caseldine, C.J., Hardardóttir, J., and Knudsen, Ó., ed., Developments in Quaternary Science: Reykjavík, Iceland, Elsevier, p. 127-151.

Herd, R.A., and Pinkerton, H., 1997, Bubble coalescence in basaltic lava: Its impacts on the evolution of bubble populations: Journal of Volcanology and Geothermal Research, v. 75, p. 137-157.

Höskuldsson, A., Sparks, R.S.J., and Carroll, M.R., 2006, Constraints on the dynamics of subglacial basalt eruptions from geological and geochemical observations at Kverkfjöll, NE-Iceland: Bulletin of Volcanology, v. 68, p. 689-701, doi: 10.1007/s00445-005-0043-4.

Jakobsson, S.P., Jónsson, J., and Shido, F., 1977, Petrology of the Western Reykjanes Peninsula, Iceland: Journal of Petrology, v. 19, p. 669-705.

Jones, J.G., 1968, Pillow lava and pahoehoe: The Journal of Geology, v. 76, p. 485-488.

Jones, J.G., 1969, Pillow Lavas as depth indicators: American Journal of Science, v. 267, p. 181-195.

Jones, J.G., 1970, Intraglacial volcanoes of the Laugervatn Region, southwest Iceland, II: The Journal of Geology, v. 78, p. 127-140.

Jull, M., and McKenzie, 1996, The effect of deglaciation of mantle melting beneath Iceland: Journal of Geophysical Research, v. 101, p. 21815-21828, doi:10.1029/96JB01308.

LeBas, M.J., LeMaitre, R.W., Streckeisen, A., and Zanettin, B., 1986, A chemical classification of volcanic rocks based on the total alkali silica diagram: Journal of Petrology, v. 27, p. 745-750.

Macdonald, G.A., 1953, Pahoehoe, aa, and block lava: American Journal of Science, v. 251, p. 163-191.

Manga, M., 1996, Waves of bubbles in basaltic magmas and lavas: Journal of Geophysical Research, v. 101, p. 17457-17465.

Marsh, B.D., 1995, Solidification fronts and magmatic evolution: Mineralogical Magazine, v. 60, p. 5-40.

Moore, J., 1975, Mechanism of formation of pillow lava: American Scientist, v. 63, p. 269-277.

Moore, J.G., and Schilling, J., 1973, Vesicles, water, and sulfur in Reykjanes Ridge basalts: Contributions to Mineralogy and Petrology, v. 41, p. 105-118.

Moore, J.G., and Calk, L.C., 1991, Degassing and differentiation in subglacial volcanoes, Iceland: Journal of Volcanology and Geothermal Research, v. 46, p. 157-180.

Pollock, M., Edwards, B., Hauksdóttir, S., Alcorn, R., and Bowman, L., 2014, Geochemical and lithostratigraphic constraints on the formation of pillow-dominated tindars from Undirhlíðar quarry, Reykjanes Peninsula, southwest Iceland: Lithos, v. 200-201, p. 317-333.

Sánchez, M.C., Sarrionandia, F., Juteau, T., and Ibarguchi, J.I.G., 2012, Structure and organization of submarine basaltic flows: Sheet flow transformation into pillow lavas in shallow submarine environments: International Journal of Earth Science, v. 101, p. 2201-2214, doi: 10.1007/s00531-012-0783-2.

Sigmarsson, O., and Steinthórsson, S., 2007, Origin of Icelandic basalts: A review of their petrology and geochemistry: Journal of Geodynamics, v. 43, p. 87-100, doi: 10.1016/j.jog.2006.09.016

Sigvaldason, G.E., Annertz, K., and Nilsson, M., 1992, Effect of glacier loading/deloading on volcanism: postglacial volcanic production rate of the Dyngjufjöll area, central Iceland: Bulletin of Volcanology, v. 54, p. 385-392, doi: 10.1007/BF00312320.

Tepley, L. (prod.), and Moore, J.G. (sci. consult.), 1974, Fire under the sea: The origin of pillow lava, (16-mm sound motion picture) Mountain View, CA: Moonlight Productions.

Thordarson, T., and Larsen, G., 2007, Volcanism in Iceland in historical time: Volcano types, eruption styles and eruptive history: Journal of Geodynamics, v. 43, p. 118-152, doi: 10.1016/j.jog.2006.09.005.

Walker, G.P.L., 1992, Morphometric study of pillow-size spectrum among pillow lavas: Bulletin of Volcanology, v. 54, p. 459-474.